Int J Adv Manuf Technol (2013) 69:1431–1441
DOI 10.1007/s00170-013-5126-3

ORIGINAL ARTICLE

Analysis of surface roughness and cutting force when turning AISI 1045 steel with grooved tools through Scott–Knott method

Robson Bruno Dutra Pereira · Durval Uchôas Braga · Frederico Ozanan Nevez · Alex Sander Chaves da Silva

Received: 4 March 2012 / Accepted: 10 June 2013 / Published online: 21 June 2013

Abstract The chip breaker presents an important role in chip control on turning operation, as well as a significant influence on cutting force, surface integrity, wear, and tool life. In this experimental study, the grooved chip breaker, feed rate, and cutting velocity influence on cutting force and surface roughness of turning process of AISI 1045 steel were investigated through a complete factorial design and the Scott–Knott method. The multiple comparison method of Scott–Knott was used to identify which combination of the factor levels was specifically different when a source of variation was statistically significant in ANOVA. This multiple comparison method was essential to choose an optimal combination between cutting conditions and chip breaker type assuring the lowest cutting force and surface roughness levels without ambiguity. The methodology proposed was effective at achieving process improvement.

Keywords Chip breaker · Cutting force · Surface roughness · Factorial design · Scott–Knott method

1 Introduction

According to Maity and Das [1], long chips curl around the tool and can pose serious hazards to the workpiece surface, the operator, and the machine–tool operations. To overcome this difficulty, a number of researchers have investigated the effective control of chip flow and breaking. Chip curl can be controlled by using an obstacle across the chip-flow direction, commonly known as chip breaker or chip former.

The chip breaker is defined as a modification of the rake face to control or break the chip, consisting of either an integral groove or an integral or attached obstruction [2].

It was investigated that the restricted contact length influence the cutting process concluding that this narrow land decreases the cutting force and temperature, and therefore increases the tool life [3]. The geometrical parameters of grooved chip breaker on chip breaking performance were investigated [4]. The chip flow mechanism on chip breaker insert was studied reporting its influence on chip curling and breaking process [5].

Analytical models of chip flow, chip curling, and chip breaking with chip breaker inserts application were developed under the concept of equivalent parameters [6, 7]. These models were studied and the chip breaker insert behavior on machining force, surface roughness, and chip-breaking process was analyzed [8]. Semi-empirical models including cutting conditions, tool geometry, and work-piece materials properties based on chip flow and chip-curling mechanisms had been developed [9].

A force decomposition model counting the influential parameters on tool wear including cutting conditions, tool geometry, and grooved-chip breaker geometry was proposed [10]. It was presented as a newly developed equivalent tool-face (ET) model for predicting the most dominant tool failure modes in turning with complex grooved chip breaker inserts [11]. The ET model was extended to correlate chip curling when machining with progressive tool-wear mechanisms in grooved chip breaker tools [12]. The performance of commercial grooved chip breakers was evaluated using a neural network [13].

R. B. D. Pereira (✉)
Instituto Federal Tecnológico do Sudeste de Minas Gerais, Rua Monteiro de Castro, 550; Bairro: Barra, 36880-000 Muriaé, Minas Gerais, Brazil
e-mail: robson.pereira@ifsudestemg.edu.br

D. U. Braga · F. O. Nevez · A. S. C. da Silva
Universidade Federal de São João del Rei, Praça Frei Orlando 170; Centro, São João del Rei 36307-352, Minas Gerais, Brazil

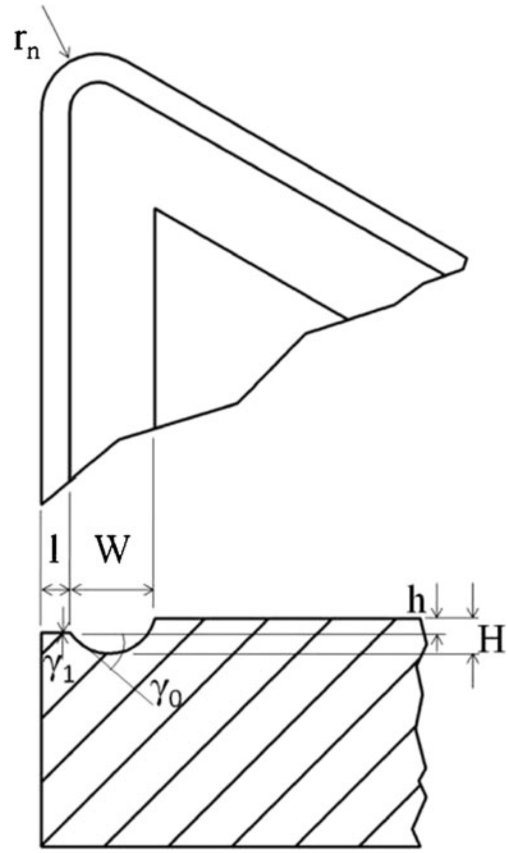

Fig. 1 Geometrical parameters of the grooved chip breaker

1.1 Grooved chip breaker

When the rear part of the tool rake face is removed so that the contact length is smaller than the natural contact length, the tool is called a restricted contact tool (insert). The use of such tools in machining has been reported as early as the 1920s. The benefits of such tools in machining are minimum compression and deformation of the chip, reduced cutting force and tool wear, etc. [14].

In the conventional grooved chip breakers, the chip flows into the groove owing to the effect of tool-restricted contact, and then is curled by the groove back-wall [7]. The knowledge of the geometrical parameters of the grooved chip breaker is essential, not only on the chip-breaking process, but it also plays an important role on the machining process efficiency.

The main geometrical parameters of a grooved chip breaker consist of the rake land length *l*, the land angle γ_1, the rake angle γ_0, the groove width *W*, the groove depth *H*, and the groove backwall height *h*, as shown in Fig. 1.

The rake land, when used in a correct way, i.e., when the restricted contact length *l* is smaller than the tool-chip natural contact length l_{nc}, presents an important key on the cutting process. This narrow land reduces cutting force and temperature and henceforth, increases the useful tool life, but on the other hand, it increases the chip curl radius, straightens the chip, and therefore results to the chip curling on the opposite direction [4].

The studies which deal with chip breaker had focused both on analytical approaches and on experimental approaches to predict the machining force components, the chip flow, chip curling and chip-breaking variables. In this experimental study, the grooved chip breaker and cutting conditions influence on cutting force F_c and on average surface roughness R_a on turning process of AISI 1045 steel were investigated through a complete factorial design and the Scott–Knott method.

2 Experimental work

2.1 Equipment and tools

Oblique cutting tests were made on a CNC turning center *ROMI GL 240M*. The cutting force F_c was measured with a tool dynamometer *Kistler 5070A* and the signal process software *Dynoware* supplied by *Kistler*. The surface roughness parameter R_a was measured by a *Surftest SJ-400 Mitutoyo*.

A tool holder with ISO code PCLNL 2020K12 from *Sandvik* C*oromant* was used in the experimental work. The side cutting edge angle χ_R, rake angle γ_0, and inclination angle λ_s were 95, −6, and −6 °, respectively. Figure 2 shows the tool holder and dynamometer set on the turning center turret.

Fig. 2 Experimental set-up

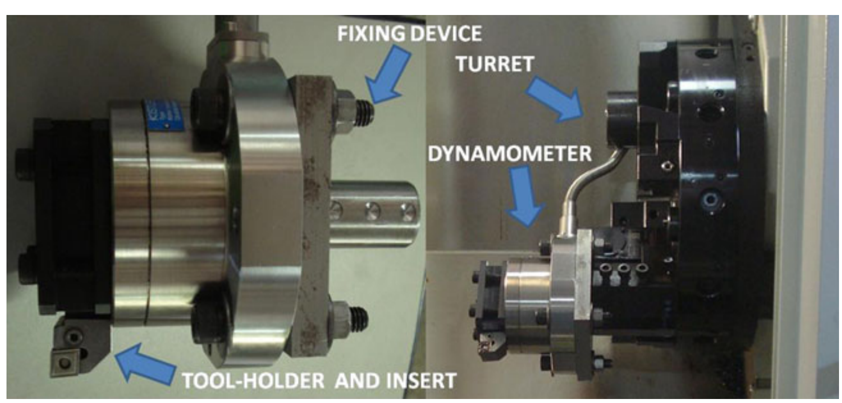

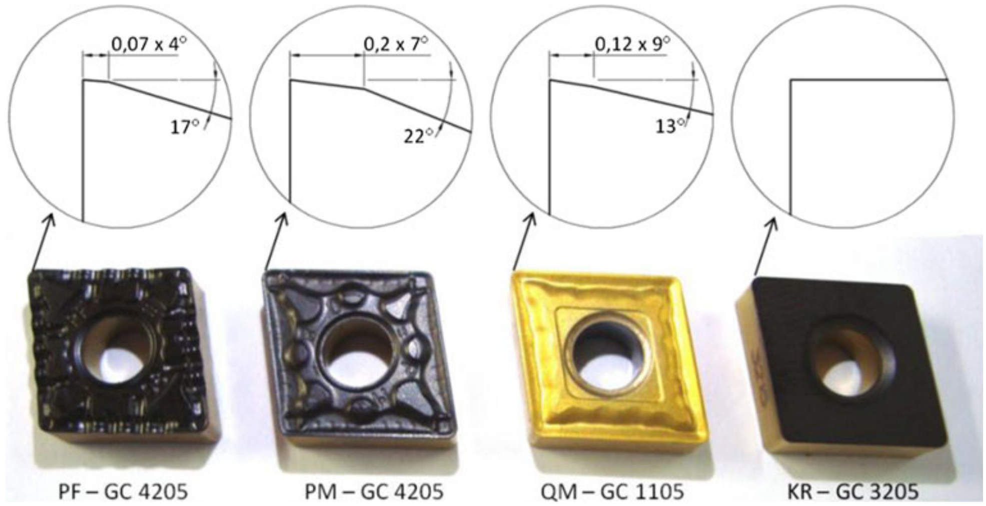

Fig. 3 Chip breaker geometries and coated carbide classes used in the experiments

Three coated carbide grooved inserts with ISO code CNMG 120408 and another coated carbide flat faced insert with ISO code CNMA 120408 were used in the experimental work. These inserts, with different groove parameters, were used to compare the performance of each one when applying different cutting conditions. The flat faced insert was used to contrast with the three grooved inserts. Figure 3 shows the schematics of the tool inserts used and identifies their respective code.

The PF grooved insert has a straight cutting edge up to 2 mm from the nose and the rest is wave. It has a very narrow land, groove only on the straight cutting edge region, curved backwall, and is appropriate for finishing. The PM-grooved insert has straight cutting edge with narrow land, groove and curved backwall. The QM-grooved insert has straight cutting edge with narrow land and wave backwall. These two inserts are appropriate to medium cutting conditions. Lastly, the flat-faced insert KR was chosen to comparison purpose.

The work material used in tests was AISI 1045 steel with a hardness average value equal to 181 BHN.

2.2 Control factors evaluated and response factors in study

No coolant was used. A constant depth of cut a_p equal to 2 mm was used in the tests. The chosen control factors in this study were the grooved chip breaker type *CB*, the feed rate per revolution of the tool *f* and the cutting velocity v_c. Table 1 summarizes these factors followed by their respective levels.

Table 1 Control factors and levels

Control factors	Unit	Levels			
Chip breaker (*CB*)	–	PF	PM	QM	KR
Feed rate (*f*)	mm/rev	0.16	0.24	0.32	
Cutting velocity (v_c)	m/min	310	380		

The factor levels chosen are between finishing and medium machining. Precisely, for the insert PF type, the depth of cut chosen is out of its specification. The intention was to assure a side flow out of the rounded region defined by the nose radius which was of 0.8 mm for all inserts. This way, the chip develops a combination between up and side curl. The PF insert was tested under the same combinations of the cutting conditions applied to the other two grooved inserts for comparison purpose.

The response variables accessed by the factorial design were the cutting force F_c and the average surface roughness R_a. The cutting force F_c was measured during each experiment and the surface roughness parameter R_a was measured in each machined surface in three different positions moved 120 ° apart from each other. Sample chips were collected from each test and a chip chart was obtained.

2.3 Experimental design

To access the control factors' influence on response variables, a factorial design was used. Factorial designs allow the estimative of the effect of a factor in different levels of the other factors, besides it, the effect of the interaction between two or more factors can be analyzed.

Through the combination of all levels of the control factors in the study, 24 tests were obtained, which were replicated three times, generating 72 tests in total ($4^1 \times 3^1 \times 2^1 \times 3$). All tests were conducted in random order.

By analysis of variance (ANOVA), all the hypotheses of non differences in treatment means were tested through the *F* test with a significance level α equal to 0.05. The normality test of Anderson–Darling and the Bartlett's test for equality of variances were performed (also with α=0.05) to assure

Table 2 Experiments and responses matrix

Run	Control factors			Responses		Run	Control factors			Responses	
	CB –	*f* (mm/rev)	*vc* (m/min)	*Ra* (μm)	*Fc* (*N*)		*CB* –	*f* (mm/rev)	*vc* (m/min)	*Ra* (μm)	*Fc* (*N*)
1	KR	0.16	310	3.71	991.03	37	PM	0.16	310	0.94	877.31
2	KR	0.16	310	4.06	974.67	38	PM	0.16	310	0.74	882.97
3	KR	0.16	310	3.85	1,008.54	39	PM	0.16	310	0.80	880.05
4	KR	0.16	380	1.18	955.14	40	PM	0.16	380	0.72	888.42
5	KR	0.16	380	1.26	959.81	41	PM	0.16	380	1.08	880.27
6	KR	0.16	380	0.90	979.96	42	PM	0.16	380	0.56	875.53
7	KR	0.24	310	1.98	1,399.52	43	PM	0.24	310	1.14	1,198.23
8	KR	0.24	310	1.70	1,370.80	44	PM	0.24	310	1.43	1,205.55
9	KR	0.24	310	3.09	1,356.21	45	PM	0.24	310	1.30	1,209.18
10	KR	0.24	380	1.83	1,342.05	46	PM	0.24	380	1.16	1,227.36
11	KR	0.24	380	2.05	1,330.01	47	PM	0.24	380	1.56	1,200.65
12	KR	0.24	380	1.59	1,350.14	48	PM	0.24	380	1.28	1,193.36
13	KR	0.32	310	3.14	1,712.83	49	PM	0.32	310	2.08	1,544.10
14	KR	0.32	310	2.57	1,727.58	50	PM	0.32	310	2.08	1,528.56
15	KR	0.32	310	3.41	1,683.15	51	PM	0.32	310	2.31	1,566.89
16	KR	0.32	380	2.81	1,687.77	52	PM	0.32	380	2.17	1,522.24
17	KR	0,32	380	2.25	1,650.20	53	PM	0.32	380	2.67	1,501.24
18	KR	0.32	380	2.73	1,690.23	54	PM	0.32	380	2.04	1,503.87
19	PF	0.16	310	1.19	902.30	55	QM	0.16	310	2.01	845.72
20	PF	0.16	310	1.02	912.67	56	QM	0.16	310	0.73	835.37
21	PF	0.16	310	1.18	916.21	57	QM	0.16	310	0.99	850.29
22	PF	0.16	380	1.04	870.88	58	QM	0.16	380	1.51	857.49
23	PF	0.16	380	0.85	894.77	59	QM	0.16	380	1.05	846.80
24	PF	0.16	380	1.11	885.12	60	QM	0.16	380	1.08	838.02
25	PF	0.24	310	2.25	1,287.40	61	QM	0.24	310	2.25	1,166.36
26	PF	0.24	310	1.94	1,309.27	62	QM	0.24	310	0.76	1,194.54
27	PF	0.24	310	1.91	1,311.10	63	QM	0.24	310	1.94	1,200.13
28	PF	0.24	380	1.76	1,280.49	64	QM	0.24	380	1.79	1,161.42
29	PF	0.24	380	2.34	1,280.55	65	QM	0.24	380	1.96	1,169.19
30	PF	0.24	380	1.93	1,286.59	66	QM	0.24	380	1.66	1,164.99
31	PF	0.32	310	3.93	1,724.08	67	QM	0.32	310	3.06	1,510.12
32	PF	0.32	310	4.23	1,721.67	68	QM	0.32	310	2.26	1,545.90
33	PF	0.32	310	2.93	1,697.23	69	QM	0.32	310	3.15	1,525.19
34	PF	0.32	380	3.22	1,674.23	70	QM	0.32	380	3.01	1,508.66
35	PF	0.32	380	3.42	1,676.26	71	QM	0.32	380	2.41	1,743.48
36	PF	0.32	380	3.13	1,686.84	72	QM	0.32	380	2.16	1,536.91

that the experimental error terms were normally distributed and the data variance were homogeneous. To obtain more details about the statistical analysis, see [15].

2.4 The Scott–Knott method

When the ANOVA indicates that the average levels of a source of variation differ, it is necessary to identify which factor levels or combination of the factors levels are specifically different. The multiple comparison method of Scott–Knott was used with this purpose. There are various procedures of multiple comparisons in the literature. However, users encounter difficulties in interpretation, such as ambiguity of results. An efficient alternative is the Scott–Knott method, which is a method of grouping means that categorizes results without ambiguity.

The Scott–Knott method procedure begins by partitioning the groups to maximize the sum of squares between groups.

Fig. 4 Residual plots for F_c

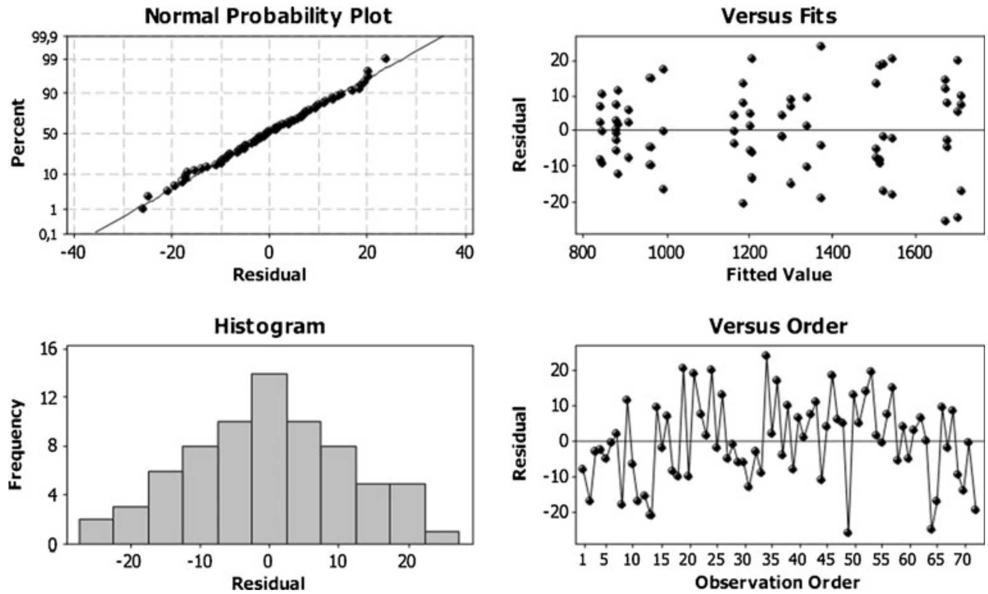

Table 3 ANOVA for cutting force F_c[a]

Source of variation	Sum of squares	DOF	Mean square	F_0	F_{tab}	*P* value
CB	310,642.42	3	103,547.47	529.49	2.80	0.000
f	6,039,482.96	2	3,019,741.48	15,441.58	3.19	0.000
v_c	6,913.19	1	6,913.19	35.35	4.04	0.000
$CB \times f$	41,636.86	6	6,939.48	35.49	2.29	0.000
$CB \times v_c$	1,692.91	3	564.30	2.89	2,80	0.045
$f \times v_c$	797.33	2	398.66	2.04	3.19	0.141
$CB \times f \times v_c$	1,473.51	6	245.58	1.26	2.29	0.295
Error	9,386.84	48	195.56	–	–	–
Total	6,412,026.00	71	–	R^2=99.85 %; R^2-aj=99.78 %		

[a] Significance level α=0.05

Fig. 5 Main effect plot for F_c

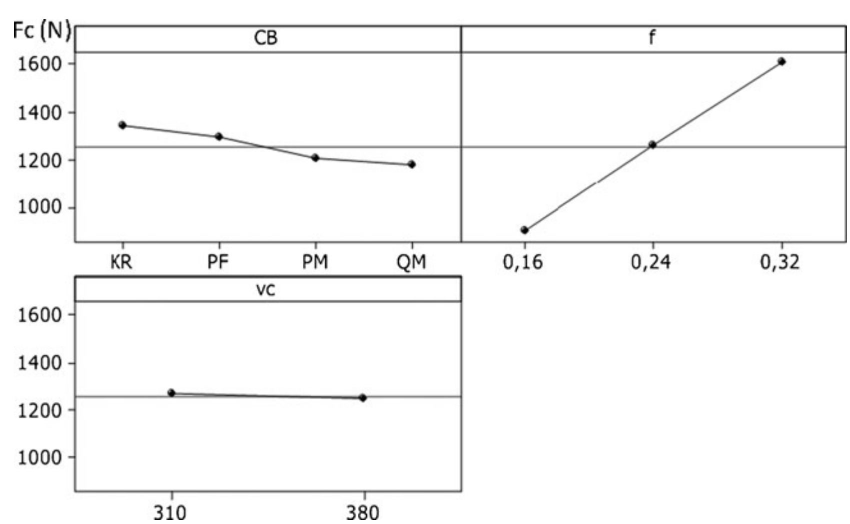

Table 4 Scott–Knott test for F_c averages. Splitting of *CB* on interaction between *CB* and *f*[a]

CB	f (mm/rev)					
	0.16		0.24		0.32	
QM	845.62	a1	1,176.11	b1	1,522.75	c1
PM	880.76	a2	1,205.72	b2	1,527.82	c1
PF	896.99	a2	1,292.57	b3	1,691.96	c2
KR	978.19	a3	1,358.12	b4	1,696.72	c2

[a] α=0.05

With the means in order, the number of possible partitions (*g*-1 partitions) is reduced.

The sum of squares B_0, is defined according to the expression:

$$B_0 = \frac{T_1^2}{K_1} + \frac{T_2^2}{K_2} - \frac{(T_1 + T_2)^2}{K_1 + K_2} \quad (1)$$

Where T_1 and T_2 are the totals of the two groups with K_1 and K_2 treatments, respectively. The maximum B_0 value obtained is used to compute the statistic λ according to the expression:

$$\lambda = \frac{\pi}{2(\pi-2)} \times \frac{B_0}{\widehat{\sigma}_0^2} \quad (2)$$

Where $\widehat{\sigma}_0^2$ is the estimator of maximum likelihood obtained by:

$$\widehat{\sigma}_0^2 = \frac{1}{g+v}\left[\sum_{i=1}^{g}\left(\overline{Y}_i - \overline{Y}\right) + v s_y^2\right] \quad (3)$$

Where $\overline{Y}_i$: mean of treatment *i* (*i*=1, 2,.... g); $\overline{Y}$: overall mean of treatments to be separated; *g* is the number of means to be separated; *v* is the number of residual degrees of freedom; s_y^2: *QMR*/*r* being *r* the number of observations that created the means to be grouped.

The statistics λ is tested by the chi square statistic (χ^2), where the condition $\lambda \geq \chi^2(\alpha; g/(\pi-2))$ indicates that the two groups are statistically different and should be tested separately for new possible divisions. On the contrary, the means are considered homogeneous and, further partitioning is therefore unnecessary. For more details about the Scott–Knott method, see [16]. All the statistical analysis was conducted using the Minitab 14 and Sisvar 5.3 softwares.

3 Results and discussion

3.1 Cutting force analysis

The output data obtained from the experiments' measurements are shown in Table 2. The Anderson–Darling test for normality of the residuals of cutting force F_c resulted in a *p* value equal to 0.985 which is larger than the significance level (α=0.05), therefore, there is not enough evidence to reject the null hypothesis assuring that the residuals follow a normal distribution.

In Fig. 4, the normal probability plot confirms that there is no deviation of the normality, the residuals plotted versus fit show that the variance is constant along the data increasing. The Bartlett's test for equality of F_c variances resulted in a *p* value equal to 0.570 which is larger than the significance level, indicating that the null hypothesis of equality of variances could not be rejected. Finally, the histogram confirms a good distribution of the residuals, and the residuals plotted versus order confirm that are not serious deviation of the independence of the residuals.

The ANOVA for F_c is shown in Table 3 with an adjusted coefficient of determination of 99.78 % assuring the excellent adjustment of the model data. From the *p* value analysis the sources of variation *CB*, *f*, v_c, and the interactions between *CB*

Fig. 6 Interaction plot for F_c

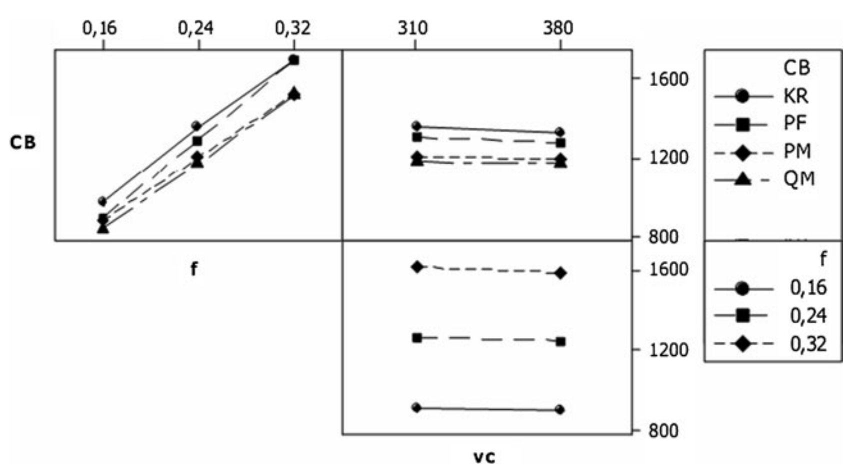

Table 5 Scott–Knott test for F_c averages. Splitting of f on interaction between CB and f[a]

f (mm/rev)	CB							
	QM		PM		PF		KR	
0.16	845.62	a1	880.76	b1	896.99	c1	978.19	d1
0.24	1,176.11	a2	1,205.72	b2	1,292.57	c2	1,358.12	d2
0.32	1,522.75	a3	1,527.82	b3	1,696.72	c3	1,691.96	d3

[a] α=0.05

and f and between CB and v_c were statistically significant (p <0.05). The feed f was the main factor of influential on the cutting force F_c, followed by chip breaker CB. Figure 5 shows the main effect plot for F_c.

To avoid that the comparisons between the means of one factor could be obscured by the interactions, the comparisons were made in the interactions which were significant on the ANOVA, i.e., fixing one factor of the interaction at a specific level and applying the Scott–Knott test on other factor average levels.

Through the Scott–Knott test, the factor CB was split in the interaction between CB and f. Table 4 summarizes the Scott–Knott test results for this interaction, where different characters mean different average response for F_c. The interaction plot, which is a graph of the average responses at each combination between the interaction of factors is shown in Fig. 6.

At CB, QM, and f level 0.16 mm/rev, the smallest average level of F_c was obtained (characters a1 at Table 4), followed by PM and PF chip breaker CB levels which presented statistically equal average levels of F_c (a2), and lastly, the KR chip-breaker level presented the highest average levels of F_c (a3). With f at level 0.24 mm/rev, the QM, PM, PF, and KR chip breaker CB levels, in increasing order, presented different average levels of F_c (b1, b2, b3, and b4 at Table 4, respectively). Finally, at f level 0.32 mm/rev, the CB levels QM and PM presented equal average level of F_c (c1) and the CB levels PF and KR presented equal average level of F_c between themselves and higher level than the first ones (c2).

Subsequently, the factor f was also split in the same interaction through the Scott–Knott test. All feed levels presented statistically significant difference on F_c average levels, independently of the CB level, confirming that when the feed f increases, the response F_c also increases. The test results are shown at Table 5.

The CB level KR presented the highest F_c levels in most tests, except for the factor f at level 0.32 mm/rev where the CB levels PF and KR presented no significant difference (c2 on Table 4). The chip breaker presence, specifically the reduction of land length l decreased the cutting force F_c, but only when it is utilized with the indicated cutting conditions which need to be in accord with its geometrical characteristics and parameters. The CB level PF, with narrow land, when applied with medium and roughing cutting conditions due the high streaming degree generated by the high ratio between feed to land length (f/l) generated undesirable chip-flow patterns occasioning high cutting force F_c levels.

In this study, the smallest cutting force levels would determine the optimal cutting conditions. Then, considering

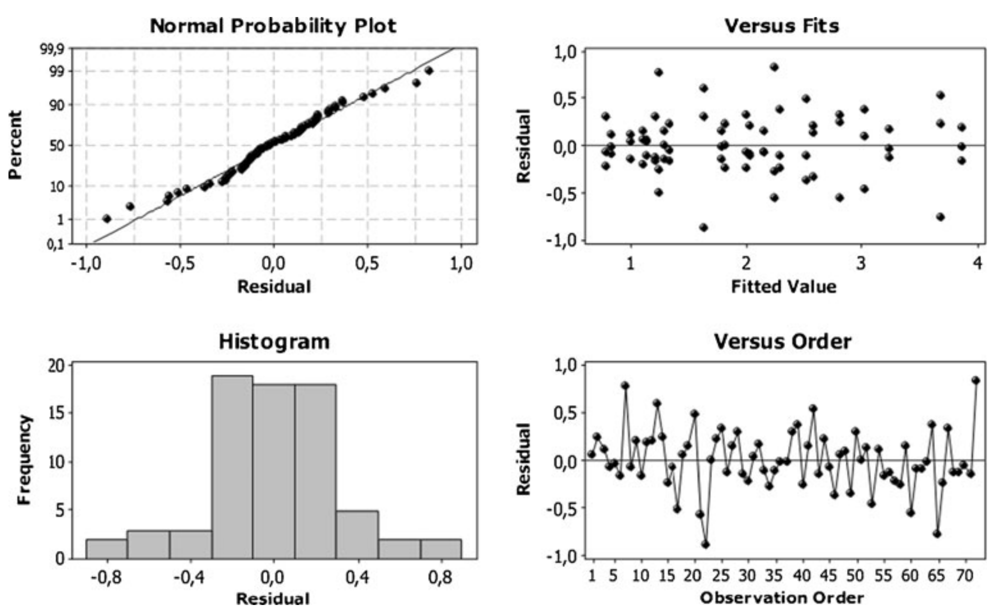

Fig. 7 Residual plots for R_a

Table 6 ANOVA for average roughness surface R_a[a]

Source of variation	Sum of squares	DOF	Mean square	F_0	F_{tab}	*p* value
CB	10.05	3	3.35	23.34	2.80	0.000
f	25.23	2	12.62	87.87	3.19	0.000
vc	2.28	1	2.28	15.87	4.04	0.000
CB x f	7.00	6	1.17	8.13	2.29	0.000
CB x vc	4.54	3	1.51	10.53	2.80	0.000
f x vc	1.44	2	0.72	5.03	3.19	0.010
CB x f x vc	4.28	6	0.71	4.96	2.29	0.001
Error	6.89	48	0.14	–	–	–
Total	61.71	71	–	R^2=88.83 %; R^2-aj=83.48 %		

[a] α=0.05

the Scott–Knott test results, the *CB* at level QM combined with *f* at level 0.16 mm/rev generated the best results for the response variable cutting force F_c. In spite of the cutting velocity which presented influence statistically significant on ANOVA, in this specific combination between *CB* and *f*, the v_c levels presented no significant difference on F_c through the Scott–Knott test.

3.2 Average surface roughness analysis R_a

The Anderson–Darling test for normality of the residuals of R_a resulted in a *p* value equal to 0.191, which is larger than the significance level (α=0.05), meaning that the residuals follow a normal distribution.

The normal probability plot in Fig. 7 confirms that there is no deviation of the normality. The residuals plotted versus fit show that the variance is constant along the data increasing. The Bartlett's test for equality of variances of R_a resulted in a *p* value equal to 0.123, which is larger than the significance level, indicating that the data presents equality of variances, which is confirmed by the versus fits. Finally, the histogram shows a good distribution of the residuals around zero, and the residuals plotted versus order confirm the independence of the residuals.

Table 6 presents the ANOVA for response factor R_a whit an adjusted coefficient of determination of 83.48 % assuring the good adjustment of the model data. The Main effect plot for R_a is shown on Fig. 8.

At tests with *CB* at level KR, v_c equal to 310 m/min and *f* equal to 0.16 mm/rev, the average surface roughness R_a was extraordinarily large because uncontrolled ribbon chips scratch the machined surface. Therefore, the interaction between the factors *CB*, *f*, and v_c was significant (ANOVA on Table 6, F_0=4.96>F_{tab}=2.29), then each variable in this interaction was split through the Scott–Knott test.

The Scott–Knott test results for splitting the *CB* levels in the interaction between the three control factors in study are shown at Table 7 followed by the interaction plot at Fig. 9.

At v_c equal to 310 m/min and *f* equal to 0.16 mm/rev, the three inserts with chip breaker presented average levels of the factor R_a statistically equal between themselves, while the flat-faced KR insert presented highest average response. At same v_c level and *f* equal to 0.24 mm/rev, the *CB* levels PM and QM presented average levels of R_a statistically equal

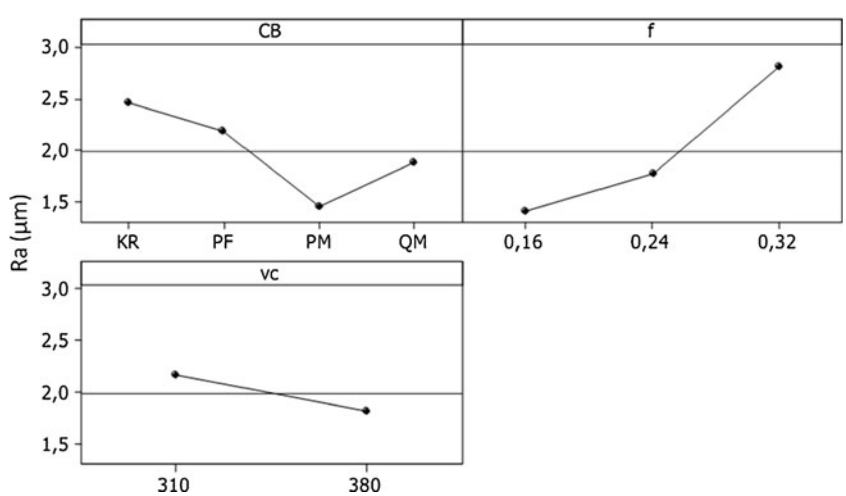

Fig. 8 Main effect plot for R_a

Table 7 Scott–Knott test for R_a averages. Splitting of *CB* on interaction between *CB*, *f*, and v_c[a]

CB	f (mm/rev)						v_c (m/min)
	0.16		0.24		0.32		
PM	0.83	a1	1.29	b1	2.16	c1	310
QM	1.24	a1	1.65	b1	2.82	c2	
PF	1.13	a1	2.03	b2	3.70	c3	
KR	3.87	a2	2.26	b2	3.04	c2	
PM	0.79	d1	1.33	e1	2.29	f1	380
QM	1.21	d1	1.80	e1	2.53	f1	
PF	1.00	d1	2.01	e1	3.26	f2	
KR	1.11	d1	1.82	e1	2.60	f1	

[a] α=0.05

between themselves and smaller than PF and KR which also presented average levels of R_a statistically equal between themselves. With v_c equal to 310 m/min and *f* equal to 0.32 m/rev, the *CB* level PM had the better behavior, i.e., the smallest average levels of R_a while QM and KR presented average levels higher than the first, equal between themselves, and smaller than the *CB* level PF, which presented the worst result.

At v_c equal to 380 m/min and *f* equal to 0.16 mm/rev, all *CB* levels presented R_a average levels statistically equal among themselves. The same happened at v_c equal to 380 m/min and *f* equal to 0.24 mm/rev. However, at the same v_c level and *f* equal to 0.32 mm/rev, the *CB* level PF presented R_a average levels higher than KR, QM, and PM which presented R_a average levels statistically equal.

The factor *f* was also split in the interaction between *CB*, *f*, and v_c through the Scott–Knott test, and the results are shown at Table 8. The *CB* levels PM and QM presented statistically significant difference only in relation to *f* level equal to 0.32 mm/rev, presenting higher R_a average levels than that obtained with *f* levels equal to 0.16 and 0.24 mm/rev which presented R_a equal average levels between themselves, independently, from the v_c levels. In the PF chip breaker *CB* case, the three feed *f* levels presented R_a statistically different and increasing average levels between themselves. Finally, the *CB* level KR at v_c 310 m/min, presented inverse behavior, in a way that the smallest *f* level presented the highest R_a level due to the generated chip forms. However, at v_c equal to 380 m/min the *CB* level KR presented similar behavior to PF in relation to splitting *f* levels.

Finally, the control factor cutting velocity v_c was also split in the interaction between CB, *f* and v_c. The Scott–Knott test results are shown at Table 9. The KR insert at feed *f* equal to 0.16mm/rev presented statistically significant difference on the average R_a levels in relation to cutting velocity v_c levels, where the lowest level (v_c=310 m/min) was responsible for the highest R_a average level, due to the undesirable generated chip forms. For all other combinations of factors *CB* and *f* levels, the v_c levels did not present statistically significant difference at R_a average levels obtained.

The optimal cutting conditions consist of the smallest average levels of the response factor R_a, which was separated by the Scott–Knott test. Therefore, the chip breaker *CB* level PM at feed *f* equal to 0.16mm/rot generated the best results for R_a. In spite of v_c having presented influence statistically significant on ANOVA, in this specific combination between

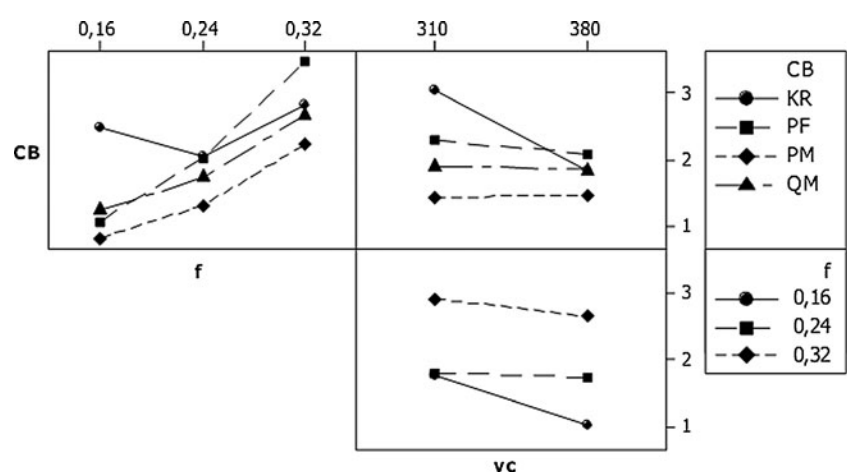

Fig. 9 Interaction plot for R_a

Table 8 Scott–Knott test for R_a averages. Splitting of f on interaction between CB, f, and v_c[a]

f (mm/rev)	CB								v_c (m/min)
	QM		PM		PF		KR		
0.16	1.24	a1	0.83	b1	1.13	c1	3.87	d3	310
0.24	1.65	a1	1.29	b1	2.03	c2	2.26	d1	
0.32	2.82	a2	2.16	b2	3.70	c3	3.04	d2	
0.16	1.21	e1	0.79	f1	1.00	g1	1.11	h1	380
0.24	1.80	e1	1.33	f1	2.01	g2	1.82	h2	
0.32	2.53	e2	2.29	f2	3.26	g3	2.60	h3	

[a] α=0.05

Table 9 Scott–Knott test for R_a averages. Splitting of v_c on interaction between CB, f, and v_c[a]

v_c (m/min)	CB								f (mm/rev)
	QM		PM		PF		KR		
380	1.21	a1	0.79	b1	1.00	c1	1.11	d1	0.16
310	1.24	a1	0.83	b1	1.13	c1	3.87	d2	
380	1.80	e1	1.33	f1	2.01	g1	1.82	h1	0.24
310	1.65	e1	1.29	f1	2.03	g1	2.26	h1	
380	2.53	i1	2.29	j1	3.26	k1	2.60	l1	0.32
310	2.82	i1	2.16	j1	3.70	k1	3.04	l1	

[a] α=0.05

CB and f, the v_c levels presented no significant difference on R_a through the Scott–Knott test.

4 Chip forms and breaking

Figure 10 shows the chip chart with chip samples collected from tests. At tests with PF and PM inserts, the chips collected were in form of short comma, while with QM insert tests, long comma chips were obtained. The obtained chips with these inserts presented a combination of side and up curling, breaking by the contact with tool flank.

At tests with flat-faced KR insert, due to the chip breaker absence, it was observed that the feed influence on chip forms. At f equal to 0.16 mm/rev, it was generated ribbon chip with v_c equal to 310 m/min and tangled chips with v_c equal to 380 m/min. At f equal to 0.24 mm/rev, helical and long comma chip forms were obtained. Finally, at f equal to 0.32 mm/rev, it was obtained long and short comma chip forms.

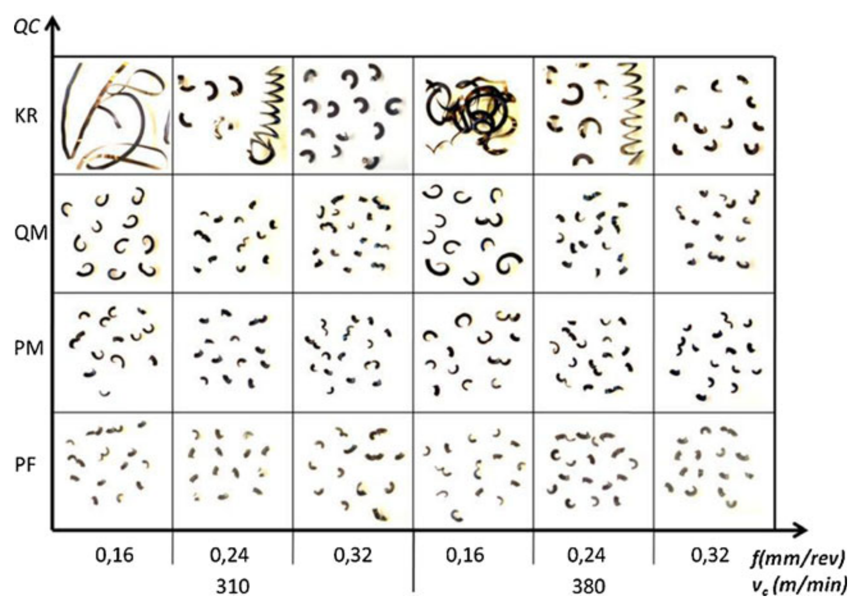

Fig. 10 Chip chart of the tests

5 Conclusions

In this study, the cutting conditions and chip-breaker profile influence were evaluated through a factorial design. By performing 72 tests, the factorial design was an effective method to evaluate the influence of each main factor and the interaction between them on cutting force F_c and average surface roughness R_a. The multiple comparison method of Scott–Knott was used to perform procedures of multiple comparisons without ambiguity showing specific differences on responses between factor levels' combinations. This multiple comparison method was essential to determine the best cutting conditions and chip breaker for the response factors in study. The methodology proposed was effective at achieving process improvement.

The optimal factor combination to obtain the smallest F_c average level was the chip breaker QM at feed equal to 0.16 mm/rev. In R_a case, the smallest average levels were obtained by the chip breaker PM at feed equal to 0.16 mm/rev.

On cutting force F_c analysis, the statistically significant interactions (CBxf and CBxv_c) justify the necessity of correcting chip breaker type application on cutting conditions which generate an ideal chip flow pattern and, consequently, decreasing the cutting force.

Despite the interaction between the three factors under analysis had been influential on R_a, the v_c influence can be justified mainly by uncontrolled ribbon chip obtained on tests with CB type KR, v_c equal to 310 m/min and f equal to 0.16 mm/rev which scratched the machined surface, generating extraordinarily large average surface roughness R_a levels.

Acknowledgements The authors gratefully acknowledge the Fundação de Amparo à Pesquisa de Minas Gerais (FAPEMIG) for financial support.

References

1. Maity KP, Das NS (1998) A slip-line solution to metal machining using a cutting tool with a step-type chip breaker. J Mater Process Technol 79:217–223
2. Boothroyd G, Knight WA (1989) Fundamentals of machining and machine tools. Marcel Dekker, New York
3. Jawahir IS (1988) The tool restricted contact effect as a major influencing factor in chip breaking: an experimental analysis. Annals of the CIRP 37:121–126
4. Fang N (1998) Influence of the geometrical parameters of the chip groove on chip breaking performance using new-style chip formers. J Mater Process Technol 74:268–275
5. Jawahir IS, Luttervelt CAV (1993) Recent developments in chip control research and applications. Annals of the CIRP 42:659–693
6. Rahman M, Seah KHW, Li XP, Zhang XD (1995) A three-dimensional model of chip flow, chip curl and chip breaking under the concept of equivalent parameters. Int J Mach Tool Manuf 35:1015–1031
7. Seah KHW, Rahman M, Li XP, Zhang XD (1996) A three-dimensional model of chip flow, chip curl and chip breaking for oblique cutting. Int J Mach Tool Manuf 36:1385–1400
8. Choi JP, Lee SJ (2001) Efficient chip breaker design by predicting the chip breaking performance. Journal of Advanced Manufacture Technology 17:489–497
9. L. Zhou (2001) Machining chip-breaking prediction with grooved inserts in steel turning. Doctor thesis, Worcester Polytechnic Institute
10. Ee KC, Balaji AK, Li PX, Jawahir IS (2001) Force decomposition model for tool-wear in turning with grooved cutting tools. Wear 249:985–994
11. Jawahir IS, Ghosh R, Balaji AK, Li PX (2000) Predictability of tool failure modes in turning with complex grooved tools using the equivalent toolface (ET) model. Wear 244:94–103
12. Ee KC, Balaji AK, Jawahir IS (2003) Progressive tool-wear mechanisms and their effects on chip-curl/chip-form in machining with grooved tools: an extended application of the equivalent toolface (ET) model. Wear 255:1404–1413
13. Kim HG, Sim JH, Kweon HJ (2009) Performance evaluation of chip breaker utilizing neural network. J Mater Process Technol 209:647–656
14. Arsecularatne JA (2004) Prediction of tool life for restricted contact and grooved tools based on equivalent feed. Int J Mach Tool Manuf 44:1271–1282
15. Montgomery DC (2001) Design and analysis of experiments. John Wiley e Sons, New York
16. Scott AJ, Knott M (1974) A cluster analysis method for grouping means in the analysis of variance. Int Biom Soc 30:507–512